The International Journal of Advanced Manufacturing Technology (2018) 98:1791–1805
https://doi.org/10.1007/s00170-018-2322-1

ORIGINAL ARTICLE

A sensitivity method to analyze the volumetric error of five-axis machine tool

Qingzhao Li[1] · Wei Wang[1] · Yunfeng Jiang[1] · Hai Li[1] · Jing Zhang[1] · Zhong Jiang[1]

Received: 4 December 2017 / Accepted: 5 June 2018 / Published online: 26 June 2018

Abstract
Geometric errors have a comprehensive influence on the volumetric error of the five-axis machine tool. The identification of the vital geometric errors that have major effect on the volumetric error is the key problem to improve the machine tool accuracy. Therefore, a sensitivity analysis method to identify the vital geometric errors is proposed in this paper. The volumetric error model of a five-axis machine tool with 41 geometric errors is established based on the multi-body system method. Through the projection of the error vectors and the introduction of the effective cutting length, LSIL and GSIL are defined as the sensitivity indices for the local and global sensitivity analysis, respectively. Simulations are conducted for the local and global sensitivity analysis in which the LSIL and GSIL are used. And the analysis results have proven the validity of the proposed sensitivity analysis method. Compared with the conventional sensitivity analysis method, the proposed sensitivity analysis method has considered the position and posture error of the cutting tool simultaneously, which is more effective and efficient. The analysis results are helpful to improve the accuracy of the five-axis machine tool.

Keywords Geometric errors · Volumetric error · Sensitivity analysis · Sensitivity indices · Accuracy of five-axis machine tool

1 Introduction

With the increasing demand of parts with geometric complexity, the five-axis machine tools are widely used in the manufacturing industry because of their advantages of better flexibility and higher efficiency. To guarantee the machining quality of the parts, high accuracy is an inevitable requirement of the five-axis machine tools, and thus, the improvement of the accuracy has received much attention. Many errors that affect the accuracy of the machine tool include geometric errors, load-induced errors, thermal-induced errors, and servo errors [1]. Among the errors, geometric errors account for the major part of the total errors and are the focus of error compensation [2–4]. Furthermore, in the review of Schwenke and Knapp [5], the thermo-mechanical errors and load-induced errors do not change the systematic of the geometric error description, which makes geometric errors more representative.

At present, the accuracy of machine tools is improved mainly through precision design and error compensation, which are both aimed at canceling the error of the cutting tool at an arbitrary point in the workspace. Precision design involves controlling the errors within a certain range by structure design, rigidity improvement, and careful assembly [6]. Compared with precision design, error compensation is much more common and economical. The most common method of error compensation is to adjust the position command via software online or offline [7–9]. Many major CNC manufacturers have realized the function of numerically compensating for the geometric errors of linear and rotary axes. Because precision design and error compensation are usually model-based, the evaluation of the error sources is essential to better improve the accuracy of machine tool. The error sources which have larger influences on the error of cutting tool are regarded as the vital ones. The improvement of accuracy of machine tool through adjusting the vital error sources is considered more effective and efficient. To identify the vital error sources, it is necessary to establish the relationship between the error sources and the error of cutting tool, and also to find an appropriate method to make the analysis.

✉ Wei Wang
wangwhit@163.com

[1] School of Mechanical and Electrical Engineering, University of Electronic Science and Technology of China, Chengdu 611731, China

The error of the cutting tool is represented by the relative deviations between actual and ideal position and posture in the workspace, i.e., the position errors in *X*, *Y*, and *Z* directions and the posture errors in *I*, *J*, and *K* directions. The volumetric error of machine tool is represented by a map of position and posture error vectors of the cutting tool over the volume concerned. And the volumetric error modeling is to establish the error mapping between the error sources and the error of the cutting tool. To date, various studies have been done on the volumetric error modeling and most methods are based on the rigid body kinematics. The D-H method is frequently applied in the robotic area. Donemz first employed the D-H method on the error modeling of machine tools, and verified the validity [10]. Fu presented one novel model of the squareness errors using the D-H method to improve the accuracy of integrated geometric errors of the machine tool [11]. In recent years, the multi-body system (MBS) method has been widely used for error modeling of machine tools [12–15]. The MBS method has the characteristics of good universality, clear physical definition, and convenient calculation. Similar to the D-H method, the homogeneous transmission matrix (HTM) is applied in the MBS method to represent the coordinate transformation between each rigid body. Considering the nonlinearity and uncertainty of errors, data fitting is suitable for the error modeling based on the measurement data [16–18]. In this paper, the MBS method is adopted for the volumetric error modeling.

Sensitivity analysis (SA) is an approach to study the impact of the model input changes on the model output. Andrea reviewed the development of SA and analyzed the requirements of SA in the context of modeling [19]. In the research on the precision design and the error compensation of machine tools, SA is widely applied to determine the vital error sources. For different purposes in the analysis of machine tool volumetric error, SA can be classified as two kinds, namely, local sensitivity analysis (LSA) and global sensitivity analysis (GSA). LSA is used to analyze the vital geometric errors when the cutting tool is at a specified point in the workspace. GSA considers the average effects of the geometric errors on the error of the cutting tool in the whole workspace. For both LSA and GSA, the definition of the sensitivity index is considered to be the key point, because the identification of the vital geometric errors is through the comparison of their corresponding sensitivity indices. In general, the greater the sensitivity index corresponding to one geometric error is, the greater its influence on the machine tool accuracy is. Wang defined the inverse position matrix as the sensitivity index in the measurement of multi-axis machine tool to investigate the accuracy [20]. Fan performed a sensitivity analysis of the 3-PRS parallel kinematic spindle platform by using the partial differential method based on the error transformation vectors and found the critical parameters to the accuracy [21]. Chen applied this same method to the sensitivity analysis of a five-axis ultra-precision machine tool in precision design [22]. Li conducted SA for precision design of the five-axis machine tool by proposing new sensitivity indices [23]. It should be noted that the method based on the error transformation vectors is valid for both LSA and GSA. GSA methods are usually model-based such as the Fourier amplitude sensitivity test, regression-based methods, and Sobol method. Cheng performed the GSA of the five-axis machine tool based on three different methods to identify the crucial geometric errors of multi-axis machine tool [24–26]. Zhang applied the MDRM method to the GSA of machine tool to better analyze the kinematic accuracy and error design [27]. Guo proposed an approach for optimizing compensation values, taking into account the GSA of position-independent geometric error [28].

Considering that the purpose of SA of the machine tool volumetric error is to determine the vital geometric errors that affect the error of cutting tool, the above work has some shortcomings to be addressed. For common SA methods for the machine tool volumetric error, the number of sensitivity indices is equal to the number of outputs of the volumetric error model. The number of outputs of the five-axis machine tool volumetric error model is six, i.e., three position errors and three posture errors in the three-dimensional workspace. It is difficult to determine the vital geometric errors when there exist so many sensitivity indices to be compared. Furthermore, the vital geometric errors identified through the SA of position error may be not effective in the improvement of the posture error. In the SA research of [22, 24–26], only position errors of the cutting tool were taken into account and the posture errors of the cutting tool are neglected. And the position errors in three directions are usually replaced by the absolute position error to conduct SA. In references [23, 28], the position errors and posture errors of the cutting tool are both considered in the SA of the machine tool volumetric error, but they were studied individually.

This paper presents a sensitivity method to analyze the machine tool volumetric error to determine the vital geometric errors of the five-axis machine tool. The identification of the vital geometric errors is based on the sensitivity index that considers both position and posture errors. The structure of this paper is arranged as follows: Sect. 2 introduces the geometric errors of the five-axis machine tool, and then, the volumetric error model is established based on the MBS method. Section 3 defines the sensitivity indices for the sensitivity method. In Sect. 4, sensitivity analyses for the five-axis machine tool volumetric errors are conducted by using the proposed sensitivity indices. Section 5 makes a discussion on the sensitivity analysis method. Finally, the article is summarized in Sect. 6.

2 Volumetric error modeling of the five-axis machine tool

2.1 Structure of the five-axis machine tool

Five-axis machine tools usually accord with three types, i.e., the type with double pivot heads (TTTRR), the type with a tilting rotary table (RRTTT), and the type with a tilting head (RTTTR). The letter T represents the translational axis and the letter R represents the rotary axis. As shown in Fig. 1, the research target in this article is the TTTRR-type five-axis machine tool with B axis and A axis. It can be described as [b X Y Z B A t] by connecting the motion axes from the bed side to the cutting tool side. The "b" denotes the bed and the "t" denotes the cutting tool in this description. The strokes of the translational axes can be expressed as $x \times y \times z = 5000 \times 2000 \times 500$ mm. The strokes of the rotary axes are both $[-30°, 30°]$.

2.2 Description of geometric errors

Geometric errors of the machine tool mainly come from manufacturing or assembly defects, which are specifically represented by the misalignment of machine's axis and the position and straightness errors of each axis. In the rigid body kinematics, these geometric errors will impact the motion accuracy of the axes, which will finally generate the error of the cutting tool. The volumetric error modeling is to establish the mapping between the geometric errors and the error of the cutting tool. Geometric errors can be divided into two kinds, i.e., the position-dependent geometric errors (PDGEs) and the position-independent geometric errors (PIGEs) [29].

PDGEs are the errors caused mainly by the defects in the components of the controlled axis itself. There can be six error components between the actual and ideal position of the axis in motion. As shown in Fig. 2, the PDGEs of each axis contain three position errors (one positioning and two straightness) and three angular errors (roll, pitch, and yaw). The three position errors can be regarded as the errors along the three ideal

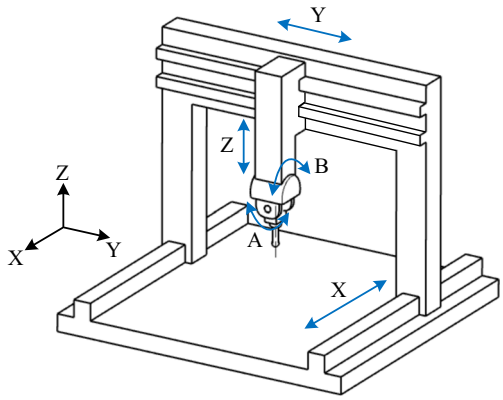

Fig. 1 The structure of five-axis machine tool

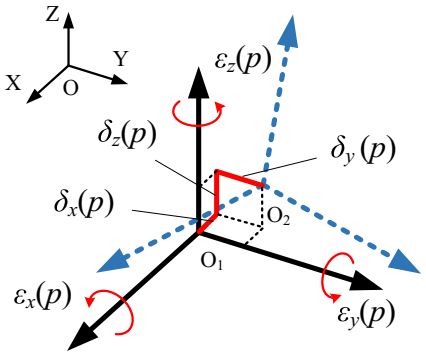

Fig. 2 The position-dependent geometric errors (PDGEs)

directions in space. And the three angular errors can be regarded as the errors around the three ideal directions in space. The PDGEs of each axis are variables that change with the axis motion. Because each axis has six PDGEs, there are total $6 \times 5 = 30$ PDGEs for the five-axis machine tool.

Compared with the PDGEs, PIGEs are generally caused by imperfections in the assembly process. The assembly defects lead the actual motion coordinate system of each axis to deviate from its ideal motion coordinate system. Because the deviations between the coordinate systems are constant, the PIGEs are fixed values. For five-axis machine tool, there are total 11 PIGEs, i.e., 3 squareness between 3 translational axes, 2 squareness of each rotary axis, and 2 position errors of each rotary axis. The PIGEs of the five-axis machine tool are described in Fig. 3, which refers to ISO 230–7 [30]. Thus, there are 30 PDGEs and 11 PIGEs; the total number of the geometric errors of the five-axis machine tool is $30 + 11 = 41$. The geometric errors of the five-axis machine tool are listed in Table 1.

2.3 The process of volumetric error modeling

The topological structure is used to describe the kinematic chain of the machine tool in the MBS method. In the topological structure of the five-axis machine tool, the bed is set as the inertial reference frame and expressed as the 0 body. According to the natural growth sequence, along the direction away from the body 0, the bodies are sequentially numbered and attached with a local coordinate system. The cutting tool is at the end of the kinematic chain. In the actual movement of the machine tool, the PDGEs of each axis affect the axis's motion in the corresponding local coordinate system. At the same time, the PIGEs impact the relative accuracy between the local coordinate systems of the adjacent bodies. Thus, based on the topological structure of the machine tool, the matrices that describe the movement of the axes and the multiplication order of these matrices can be determined. The topological structure of the five-axis machine tool is displayed in Fig. 4. The errors of the spindle and the cutting tool are neglected in the volumetric error modeling.

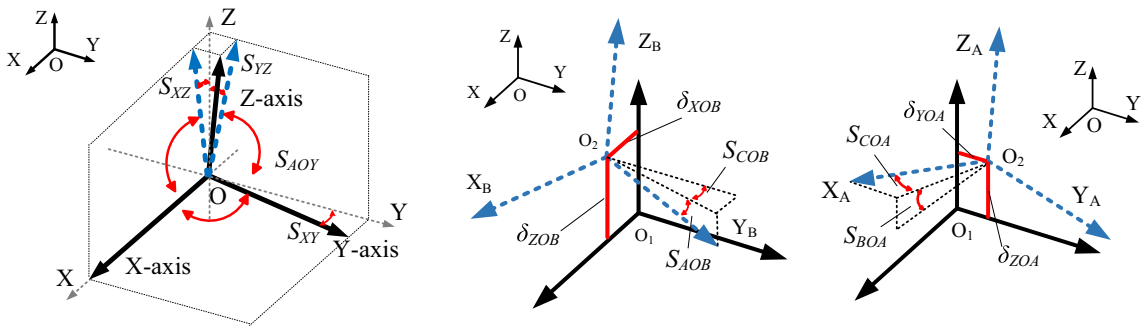

(a) The PIGEs of 3 translational axes (b) The PIGEs of B-axis (c) The PIGEs of A-axis

Fig. 3 The position-independent geometric errors (PIGEs)

The matrix $\boldsymbol{T}_{actual}{}^{i}_{j}$ is used to express the actual movement transformation between the adjacent rigid bodies i and j, given by Eq. (1). $T_{actual}{}^{i}_{j}$ is the product of the PIGE transformation matrix $\boldsymbol{PI}^{i}_{j}$, the ideal movement transformation matrix $\boldsymbol{T}^{i}_{j}$, and the PDGE transformation matrix $\boldsymbol{PD}^{i}_{j}$. Next, according to the topological structure of the five-axis machine tool, the actual movement of the cutting tool can be calculated through the product of the matrices $\boldsymbol{T}_{actual}{}^{i}_{j}$ between every two rigid bodies. It is obvious that in the process of calculation of the actual movement of the cutting tool, the 41 geometric errors are all involved. Similarly, the ideal movement of the cutting tool can also be calculated through the product of the ideal movement transformation matrices without considering these 41 geometric errors. Therefore, by comparing the actual and ideal movement of the cutting tool, the volumetric error of the cutting tool can be finally obtained.

$$\boldsymbol{T}_{actual}{}^{i}_{j} = \boldsymbol{PI}^{i}_{j}\cdot\boldsymbol{T}^{i}_{j}\cdot\boldsymbol{PD}^{i}_{j} \tag{1}$$

Based on Eq. (1) and the descriptions of the geometric errors, the actual movement transformation between adjacent rigid bodies can be calculated as listed from Eqs. (2)–(6).

$$\boldsymbol{T}^{1}_{0\,actual} = \boldsymbol{T}^{1}_{0}\boldsymbol{PD}^{1}_{0} = \begin{bmatrix} 1 & 0 & 0 & x \\ 0 & 1 & 0 & 0 \\ 0 & 0 & 1 & 0 \\ 0 & 0 & 0 & 1 \end{bmatrix} \begin{bmatrix} 1 & -\varepsilon_z(x) & \varepsilon_y(x) & \delta_x(x) \\ \varepsilon_z(x) & 1 & -\varepsilon_x(x) & \delta_y(x) \\ -\varepsilon_y(x) & \varepsilon_x(x) & 1 & \delta_z(x) \\ 0 & 0 & 0 & 1 \end{bmatrix} \tag{2}$$

$$\boldsymbol{T}^{2}_{1\,actual} = \boldsymbol{PI}^{2}_{1}\boldsymbol{T}^{2}_{1}\boldsymbol{PD}^{2}_{1} = \begin{bmatrix} 1 & -S_{xy} & 0 & 0 \\ S_{xy} & 1 & 0 & 0 \\ 0 & 0 & 1 & 0 \\ 0 & 0 & 0 & 1 \end{bmatrix} \begin{bmatrix} 1 & 0 & 0 & 0 \\ 0 & 1 & 0 & y \\ 0 & 0 & 1 & 0 \\ 0 & 0 & 0 & 1 \end{bmatrix} \begin{bmatrix} 1 & -\varepsilon_z(y) & \varepsilon_y(y) & \delta_x(y) \\ \varepsilon_z(y) & 1 & -\varepsilon_x(y) & \delta_y(y) \\ -\varepsilon_y(y) & \varepsilon_x(y) & 1 & \delta_z(y) \\ 0 & 0 & 0 & 1 \end{bmatrix} \tag{3}$$

$$\boldsymbol{T}^{3}_{2\,actual} = \boldsymbol{PI}^{3}_{2}\boldsymbol{T}^{3}_{2}\boldsymbol{PD}^{3}_{2} = \begin{bmatrix} 1 & 0 & S_{xz} & 0 \\ 0 & 1 & -S_{yz} & 0 \\ -S_{xz} & S_{yz} & 1 & 0 \\ 0 & 0 & 0 & 1 \end{bmatrix} \begin{bmatrix} 1 & 0 & 0 & 0 \\ 0 & 1 & 0 & 0 \\ 0 & 0 & 1 & z \\ 0 & 0 & 0 & 1 \end{bmatrix} \begin{bmatrix} 1 & -\varepsilon_z(z) & \varepsilon_y(z) & \delta_x(z) \\ \varepsilon_z(z) & 1 & \varepsilon_x(z) & \delta_y(z) \\ -\varepsilon_y(z) & \varepsilon_x(z) & 1 & \delta_z(z) \\ 0 & 0 & 0 & 1 \end{bmatrix} \tag{4}$$

$$\boldsymbol{T}^{4}_{3\,actual} = \boldsymbol{PI}^{4}_{3}\boldsymbol{T}^{4}_{3}\boldsymbol{PD}^{4}_{3} = \begin{bmatrix} 1 & -S_{AOB} & 0 & \delta_{XOB} \\ S_{AOB} & 1 & -S_{COB} & 0 \\ 0 & S_{COB} & 1 & \delta_{ZOB} \\ 0 & 0 & 0 & 1 \end{bmatrix} \begin{bmatrix} \cos B & 0 & \sin B & 0 \\ 0 & 1 & 0 & 0 \\ -\sin B & 0 & \cos B & 0 \\ 0 & 0 & 0 & 1 \end{bmatrix} \begin{bmatrix} 1 & -\varepsilon_z(B) & \varepsilon_y(B) & \delta_x(B) \\ \varepsilon_z(B) & 1 & -\varepsilon_x(B) & \delta_y(B) \\ -\varepsilon_y(B) & \varepsilon_x(B) & 1 & \delta_z(B) \\ 0 & 0 & 0 & 1 \end{bmatrix} \tag{5}$$

$$\boldsymbol{T}^{5}_{4\,actual} = \boldsymbol{PI}^{5}_{4}\boldsymbol{T}^{5}_{4}\boldsymbol{PD}^{5}_{4} = \begin{bmatrix} 1 & -S_{BOA} & S_{COA} & 0 \\ S_{BOA} & 1 & 0 & \delta_{YOA} \\ -S_{COA} & 0 & 1 & \delta_{ZOA} \\ 0 & 0 & 0 & 1 \end{bmatrix} \begin{bmatrix} 1 & 0 & 0 & 0 \\ 0 & \cos A & -\sin A & 0 \\ 0 & \sin A & \cos A & 0 \\ 0 & 0 & 0 & 1 \end{bmatrix} \begin{bmatrix} 1 & -\varepsilon_z(A) & \varepsilon_y(A) & \delta_x(A) \\ \varepsilon_z(A) & 1 & -\varepsilon_x(A) & \delta_y(A) \\ -\varepsilon_y(A) & \varepsilon_x(A) & 1 & \delta_z(A) \\ 0 & 0 & 0 & 1 \end{bmatrix} \tag{6}$$

Table 1 Geometric errors of the five-axis machine tool

Geometric errors		Symbols
PDGEs	*X* axis	$\varepsilon_x(x)$, $\varepsilon_y(x)$, $\varepsilon_z(x)$, $\delta_x(x)$, $\delta_y(x)$, $\delta_z(x)$
	Y axis	$\varepsilon_x(y)$, $\varepsilon_y(y)$, $\varepsilon_z(y)$, $\delta_x(y)$, $\delta_y(y)$, $\delta_z(y)$
	Z axis	$\varepsilon_x(z)$, $\varepsilon_y(z)$, $\varepsilon_z(z)$, $\delta_x(z)$, $\delta_y(z)$, $\delta_z(z)$
	B axis	$\varepsilon_x(B)$, $\varepsilon_y(B)$, $\varepsilon_z(B)$, $\delta_x(B)$, $\delta_y(B)$, $\delta_z(B)$
	A axis	$\varepsilon_x(A)$, $\varepsilon_y(A)$, $\varepsilon_z(A)$, $\delta_x(A)$, $\delta_y(A)$, $\delta_z(A)$
PIGEs		S_{xy}, S_{xz}, S_{yz}, δ_{XOB}, δ_{ZOB}, S_{AOB}, S_{COB}, δ_{YOA}, δ_{ZOA}, S_{BOA}, S_{COA}

When the length between the cutting tool tip and the rotation center of the machine tool is measured as L, the initial position of the cutting tool tip $\boldsymbol{P_t}$ can be defined as $[0, 0, -L, 1]^T$. In addition, the initial posture of the cutting tool $\boldsymbol{V_t}$ can be defined as $[0, 0, -1, 0]^T$. Based on the actual movement transformation matrices and the definitions of $\boldsymbol{P_t}$ and $\boldsymbol{V_t}$ above, the actual and ideal movement of the cutting tool can be expressed as in Eqs. (7) and (8).

$$\begin{cases} \boldsymbol{P}_{actual} = \boldsymbol{T}_{actual}{}_0^1\boldsymbol{T}_{actual}{}_1^2\boldsymbol{T}_{actual}{}_2^3\boldsymbol{T}_{actual}{}_3^4\boldsymbol{T}_{actual}{}_4^5\boldsymbol{P}_t \\ \boldsymbol{P}_{ideal} = \boldsymbol{T}_0^1\boldsymbol{T}_1^2\boldsymbol{T}_2^3\boldsymbol{T}_3^4\boldsymbol{T}_4^5\boldsymbol{P}_t \end{cases} \tag{7}$$

$$\begin{cases} \boldsymbol{V}_{actual} = \boldsymbol{T}_{actual}{}_0^1\boldsymbol{T}_{actual}{}_1^2\boldsymbol{T}_{actual}{}_2^3\boldsymbol{T}_{actual}{}_3^4\boldsymbol{T}_{actual}{}_4^5\boldsymbol{V}_t \\ \boldsymbol{V}_{ideal} = \boldsymbol{T}_0^1\boldsymbol{T}_1^2\boldsymbol{T}_2^3\boldsymbol{T}_3^4\boldsymbol{T}_4^5\boldsymbol{V}_t \end{cases} \tag{8}$$

Thus, through the comparison of the actual and ideal positions of the cutting tool, the volumetric errors of the cutting tool can be expressed as Eq. (9), including the position and posture error.

$$\begin{cases} \boldsymbol{P}_{err} = \boldsymbol{P}_{actual} - \boldsymbol{P}_{ideal} \\ \boldsymbol{V}_{err} = \boldsymbol{V}_{actual} - \boldsymbol{V}_{ideal} \end{cases} \tag{9}$$

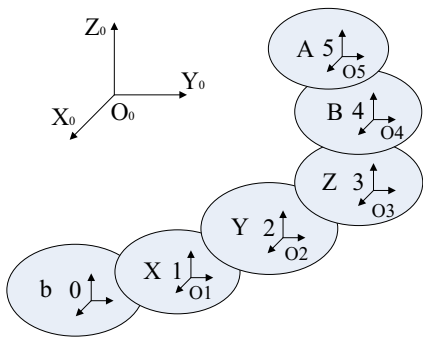

Fig. 4 The topological structure of the five-axis machine tool

3 Definition of the sensitivity indices

3.1 Introduction of the sensitivity indices

The geometric errors have a comprehensive influence on the error of the cutting tool. Among these geometric errors, some geometric errors have greater impacts on the error of the cutting tool than the others. Such geometric errors are defined as vital geometric errors compared with the other geometric errors. In order to evaluate the influence of each geometric error on the error of the cutting tool and then determine the vital geometric errors, the SA is adopted. In the approach of the SA, the definition of sensitivity index has a decisive influence on the result of the SA. Through the mathematical definition of the sensitivity index, the effect of each geometric error on the error of the cutting tool can be evaluated by its corresponding calculated sensitivity index. Then, by comparing the sensitivity indices corresponding to the geometric errors, the vital geometric errors that have significant impact on the error of the cutting tool can be identified. In general, the larger the sensitivity index corresponding to the geometric error is, the greater the influence of this geometric error on the error of the cutting tool will be. Therefore, defining reasonable sensitivity indices is critical in SA.

As mentioned in Sect. 1, sensitivity indices in the SA of the machine tools are usually defined by the operation of the partial differentiation method. In reference [23], the definitions of local sensitivity index (LSI) and global sensitivity index (GSI) are introduced. The shortage for this method of definition is that LSIs and GSIs must be equal to the number of the outputs of the volumetric error model. Considering that the output of the volumetric error model contains three position errors and three posture errors of the cutting tool, it is difficult to identify the vital geometric errors by comparing as many as six LSIs and GSIs. The reference [23] proposed three new definitions of sensitivity indices, and reduced the number of each geometric error sensitivity indices into two, i.e., one for the position error and the other for the posture error. However, the demand to use only one sensitivity index to determine the vital geometric errors that are both effective for the position and the posture errors of the cutting tool is still not met. The improvement of the machine tool volumetric accuracy can be regarded as reducing the difference between the actual and ideal position of the cutting tool, including the position and posture error. Therefore, in this paper, the new definitions of the sensitivity indices are proposed by considering the position and the posture error of the cutting tool simultaneously.

3.2 The relationship between the position error and the posture error

The error of the cutting tool is affected by the comprehensive effects of the 41 geometric errors. By differentiating Eq. (9)

with respect to geometric errors and the error of the cutting tool, the relationship between the error of the cutting tool and the geometric errors can be obtained.

$$\boldsymbol{P_{err}} = \sum_{i=1}^{41} \boldsymbol{J}_i E_i \tag{10}$$

$$\boldsymbol{V_{err}} = \sum_{i=1}^{41} \boldsymbol{K_i} E_i \tag{11}$$

With

$$\boldsymbol{P_{err}} = [P_{errX}, P_{errY}, P_{errZ}]^{\mathrm{T}}$$

$$\boldsymbol{J_i} = \left[\frac{\partial P_{errX}}{\partial E_i}, \frac{\partial P_{errY}}{\partial E_i}, \frac{\partial P_{errZ}}{\partial E_i}\right]^{\mathrm{T}}$$

$$\boldsymbol{V_{err}} = [V_{errI}, V_{errJ}, V_{errK}]^{\mathrm{T}}$$

$$\boldsymbol{K_i} = \left[\frac{\partial V_{errI}}{\partial E_i}, \frac{\partial V_{errJ}}{\partial E_i}, \frac{\partial V_{errK}}{\partial E_i}\right]^{\mathrm{T}}$$

where P_{errX}, P_{errY}, P_{errZ}, and V_{errX}, V_{errY}, V_{errZ} represent the position and posture error components of the cutting tool in three directions of the workspace, respectively. E represents the geometric errors.

Some geometric errors have the same position error transformation vector $\boldsymbol{J}$, which means that they have the same effects on the error of the cutting tool. This will be discussed later in this section. By putting the geometric errors with the same error transformation vector into the same group, the error transformation vectors of the geometric errors are listed in Table 2.

For most of the studies for the volumetric error of the five-axis machine tool, the position and posture error of the cutting tool are usually analyzed separately. In fact, the posture error is determined directly by the position error. The analysis is as follows: suppose the initial position of the cutting tool is $\mathbf{O_1P_t}$ as shown in Fig. 5. O_1 represents the ideal rotation center position of the five-axis machine tool, and P_t denotes the initial position of the cutting tool tip. When only considering the position error induced in Y direction, the actual position of $\mathbf{O_1P_t}$ will change to $\mathbf{O_2P_a}$. $\mathbf{m}$ and $\mathbf{n}$ represent the position error vectors for O_1 and P_t relative to the initial positions, respectively. Translating the position of O_2 to coincide with O_1, the position of the cutting tool tip will be P_{a1}. Obviously, the angle θ between $\mathbf{O_1P_t}$ and $\mathbf{O_1P_{a1}}$ is the change of the posture caused by the position error. The vector $\mathbf{v}$ that results in the change of the posture is the difference of $\mathbf{m}$ and $\mathbf{n}$, which can also be expressed as the product of the posture error vector in J direction and the length of $\mathbf{O_1P_t}$. Therefore, we can see that the posture error is directly influenced by position error.

Taking the angular error $\varepsilon_x(x)$ of the X axis as an example, its position error transformation vector is $[0, L\cos A\cos B\text{-}Z, Y + L\sin A]^{\mathrm{T}}$. If the length between the cutting tool tip and the rotation center is L_1 and the current position of each axis is $[X_1, Y_1, Z_1, A_1, B_1]$, the position errors of the rotation center

Table 2 The error transformation vectors of the geometric errors

No.	Geometric errors	The position error transformation vector $\boldsymbol{J}$			The posture error transformation vector $\boldsymbol{K}$		
		X	Y	Z	I	J	K
1	$\varepsilon_x(x)$, S_{yz}	0	$L\cos A\cos B\text{-}Z$	$Y + L\sin A$	0	$\cos A\cos B$	$\sin A$
2	$\varepsilon_y(x)$, $\varepsilon_y(y)$, S_{xz}	$Z\text{-}L\cos A\cos B$	0	$L\cos A\sin B$	$-\cos A\cos B$	0	$\cos A\sin B$
3	$\varepsilon_z(x)$, S_{xy}	$-Y\text{-}L\sin A$	$-L\cos A\sin B$	0	$-\sin A$	$-\cos A\sin B$	0
4	$\delta_x(x)$, $\delta_x(y)$, $\delta_x(z)$, δ_{XOB}	1	0	0	0	0	0
5	$\delta_y(x)$, $\delta_y(y)$, $\delta_y(z)$, $\delta_y(B)$, δ_{YOA}	0	1	0	0	0	0
6	$\delta_z(x)$, $\delta_z(y)$, $\delta_z(z)$, δ_{ZOB}	0	0	1	0	0	0
7	$\varepsilon_x(y)$	0	$L\cos A\cos B\text{-}Z$	$L\sin A$	0	$\cos A\cos B$	$\sin A$
8	$\varepsilon_z(y)$, $\varepsilon_z(z)$, S_{AOB}	$-L\sin A$	$-L\cos A\sin B$	0	$-\sin A$	$\cos A\sin B$	0
9	$\varepsilon_x(z)$, S_{COB}	0	$L\cos A\cos B$	$L\sin A$	0	$\cos A\cos B$	$\sin A$
10	$\varepsilon_y(z)$, $\varepsilon_y(B)$, S_{COA}	$-L\cos A\cos B$	0	$L\cos A\sin B$	$-\cos A\cos B$	0	$\cos A\sin B$
11	$\varepsilon_x(B)$, $\varepsilon_x(A)$	$L\sin A\sin B$	$L\cos A$	$L\sin A\cos B$	$\sin A\sin B$	$\cos A$	$\sin A\cos B$
12	$\varepsilon_z(B)$, S_{BOA}	$-L\sin A\cos B$	0	$L\sin A\sin B$	$-\sin A\cos B$	0	$\sin A\sin B$
13	$\delta_x(B)$, $\delta_x(A)$	$\cos B$	0	$-\sin B$	0	0	0
14	$\delta_z(B)$, δ_{ZOA}	$\sin B$	0	$\cos B$	0	0	0
15	$\varepsilon_y(A)$	$-L\cos B$	0	$L\sin B$	$-\cos B$	0	$\sin B$
16	$\varepsilon_z(A)$	0	0	0	0	0	0
17	$\delta_y(A)$	$\sin A\sin B$	$\cos A$	$\sin A\cos B$	0	0	0
18	$\delta_z(A)$	$\cos A\sin B$	$-\sin A$	$\cos A\cos B$	0	0	0

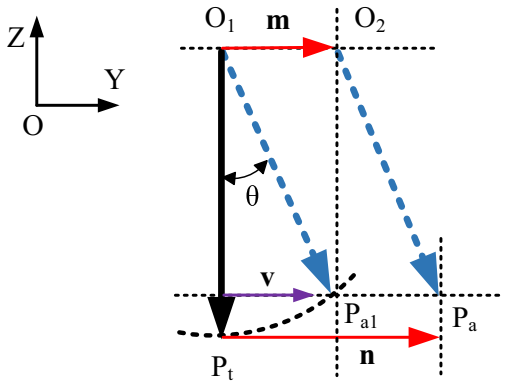

Fig. 5 The relationships between the position and posture error vectors

and the cutting tool tip in Y direction caused by $\varepsilon_x(x)$ are $-Z_1\varepsilon_x(x)$ and $(L_1\cos A_1\cos B_1\text{-}Z_1)\varepsilon_x(x)$, respectively. The vector **v** can be calculated as $[0, L_1\cos A_1\cos B_1\varepsilon_x(x)]^{\mathrm{T}}$. As the vector **v** can also be expressed as the product of the posture error vector in J direction and L_1, the posture error vector in J direction can be derived as $[0, \cos A_1\cos B_1\varepsilon_x(x)]^{\mathrm{T}}$. Thus, the posture error transformation vector of $\varepsilon_x(x)$ in the J direction can be deduced as $\cos A_1\cos B_1$, which coincides with the result listed in Table 2.

The above analysis has validated that the geometric errors with the same position error transformation vector $\boldsymbol{J}$ have the same effects on the position and posture error of the cutting tool. But it should be noted that the geometric errors with the same posture error transformation vector $\boldsymbol{K}$ may not have the same effects on the position error of the cutting tool. Because the position error vectors **m** and **n** resulting from different geometric errors may also have the same difference that generates the same posture error of the cutting tool. For example, as listed in Table 2, the first group of geometric errors and the seventh group of geometric errors have the same posture error transformation vectors, but their position error transformation vectors are different. It should also be noted that, if the position error transformation vector of one geometric error is independent of the length L, it has no influence on the posture error of the cutting tool, as seen in Table 2. In addition, there is a special geometric error $\varepsilon_z(A)$ that has no effect on both the position and posture error of the cutting tool.

3.3 The new definitions of the sensitivity indices

The reason that the conventional sensitivity analysis methods contain too many sensitivity indices is that the error components in three directions of the position and posture error of the cutting tool are considered separately. To reduce the number of sensitivity indices into only one, the new sensitivity index should contain all these considerations. Based on the analysis in Sect. 3.2, when the cutting tool length is introduced, the influence of the geometric errors on the error of the cutting tool can be represented as the influence on the position error of the cutting tool. Therefore, the sensitivity indices can be defined by applying the position error transformation vectors of the geometric errors.

By means of the error vector projection, the components of the position error of the cutting tool in three directions of the workspace can be uniformly considered. As illustrated in Fig. 6, the position error vector of the cutting tool $\boldsymbol{P_{err}}$ is formed under the common influence of the position error vectors $\boldsymbol{J_iE_i}$ caused by 41 geometric errors. The effect of each geometric error on $\boldsymbol{P_{err}}$ can be described as the projection of its resulting position error $\boldsymbol{J_iE_i}$ vector on $\boldsymbol{P_{err}}$, which depends upon the size of the projection. The projection size w_i is expressed as in Eq. (12), where $\boldsymbol{P_{err,i}}$ represents the projection of $\boldsymbol{J_iE_i}$ on $\boldsymbol{P_{err}}$.

$$\begin{cases} \boldsymbol{P}_{err,i} = \dfrac{\boldsymbol{J}_i\boldsymbol{E}_i\cdot\boldsymbol{P}_{err}}{|\boldsymbol{J}_i\boldsymbol{E}_i||\boldsymbol{P}_{err}|}\boldsymbol{J}_i\boldsymbol{E}_i \\ w_i = \left|\boldsymbol{P}_{err,i}\right| \end{cases} \tag{12}$$

The value of w_i is related to the position of each axis and the length L. When the position of the cutting tool in the workspace is determined, the position of each axis is also confirmed. Thus, w_i can be regarded as the function of the length L. The effective cutting length L_E is introduced in the definition of W_i as displayed in Eq. (13), where L_0 denotes the length between the rotation center and the cutting tool tip.

$$W_i = \int_{L_0-L_E}^{L_0} \frac{w_i}{|\boldsymbol{P_{err}}|}\mathrm{d}L \tag{13}$$

The definition of W_i can be described in Fig. 7. The $\mathbf{O_1P_t}$ is the effective cutting region of the cutting tool, and its length is L_E. Influenced by the geometric errors, the actual position of $\mathbf{O_1P_t}$ turns to $\mathbf{O_{1a}P_{1a}}$. W_i is integral of the ratio of w_i and the value of $\boldsymbol{P_{err}}$ over the length of $\mathbf{O_1P_t}$, which represents the influence of each geometric error on the position errors over the whole effective cutting region of the cutting tool.

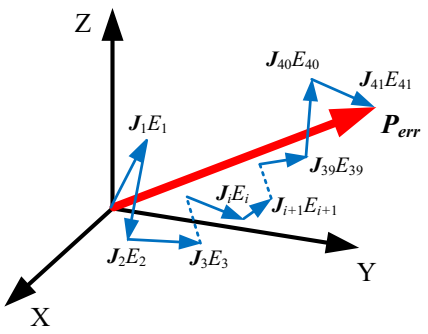

Fig. 6 The relationship between $\boldsymbol{P_{err}}$ and $\boldsymbol{J_iE_i}$

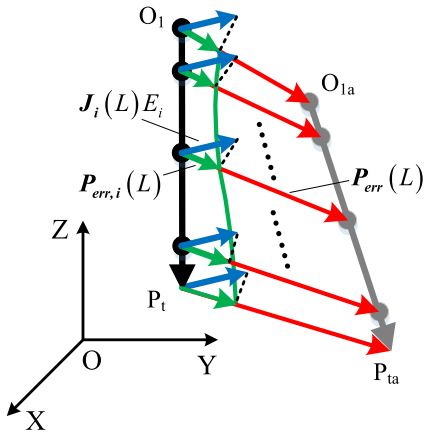

Fig. 7 The definition of W_i

According to the analysis in Sect. 3.2, it can be known that W_i includes the considerations of both the position and posture error of the cutting tool.

In the machining process, the influence of the error of the cutting tool on the workpiece depends on the relative positions of the workpiece surface and the cutting tool. Figure 8a shows the projection of the position errors over the effective cutting region onto the end plane of the cutting tool. Obviously, the actual cutting tool position has different influence on the machining error of surface *A* and surface *B*. Thus, in the LSA, the position error of the cutting tool must be projected to the normal plane of the workpiece surface to reflect its real effect. As shown in Fig. 8b, there is a big difference when the error of the cutting tool is projected on different planes. When the normal vector of the workpiece surface is $\boldsymbol{N}$, the sensitivity index in the LSA can be finally expressed as the product of W_i and $\boldsymbol{N}$. Corresponding to the previous LSIs in LSA, $W_i\boldsymbol{N}$ is defined as the sensitivity index named LSIL for the LSA in this paper.

For the GSA of the five-axis machine tool, the sensitivity index G_i can be defined as the integral of W_i over the whole workspace. The definition of G_i can be understood as the average effect of each geometric error on the error of the cutting tool at every possible point in the workspace. The expression of G_i is given in Eq. (14), where s represents the whole workspace. To distinguish G_i from the previous GSIs in GSA, the G_i is named GSIL.

$$G_i = \frac{\int_S W_i \mathrm{d}s}{\int_S \mathrm{d}s} \tag{14}$$

4 Sensitivity analysis of volumetric errors

In the sensitivity analysis of the five-axis machine tool volumetric error, the geometric errors are the only considered error sources. The geometric errors analyzed in this paper are quasi-static and are considered as systematic errors of the five-axis machine tool. The dynamical fluctuations caused by axis acceleration, dynamic load-induced errors, and thermal errors are not taken into consideration. In the numerical simulation for both LSA and GSA, the 41 geometric errors are set to the same value (0.1 μm for the position errors and 0.1 μrad for the angular errors). Note that the PDGEs should vary with the axes' positions, but here, they are set as fixed values to simplify the simulation. The LSA for the machining error of a cone is conducted to test the effectiveness of the proposed LSA method using the sensitivity index LSIL. Similarly, the GSA for the five-axis machine tool is conducted to validate the GSA method in which the sensitivity index GSIL is applied.

4.1 Local sensitivity analysis

The machining error of a 1/4 cone is selected as the target for the sensitivity analysis. The parameters of the 1/4 cone are listed as follows: diameter of 400 mm, height of 30 mm, and the angle between the busbar and the bottom plane of 60°. Place the 1/4 cone in the *XY* plane at $Z = 0$ and make its geometric center coincide with the machining center. The length between the rotation center and the cutting tool tip is set as

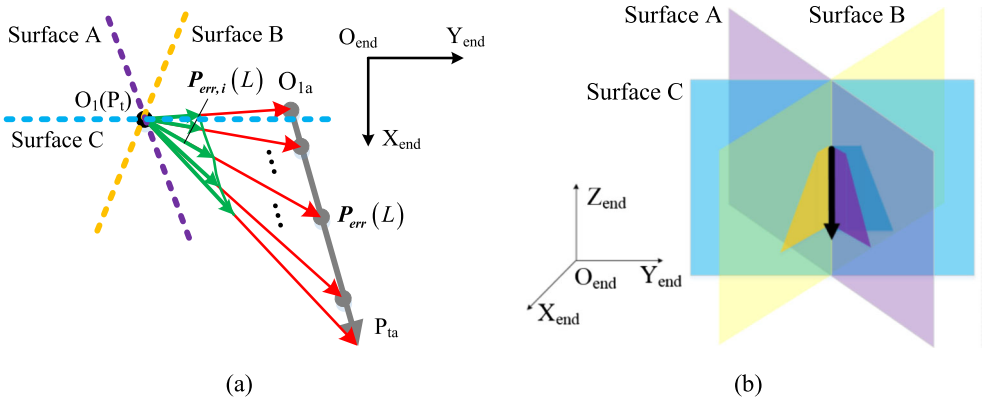

Fig. 8 The effect of cutting tool error on the workpiece surface

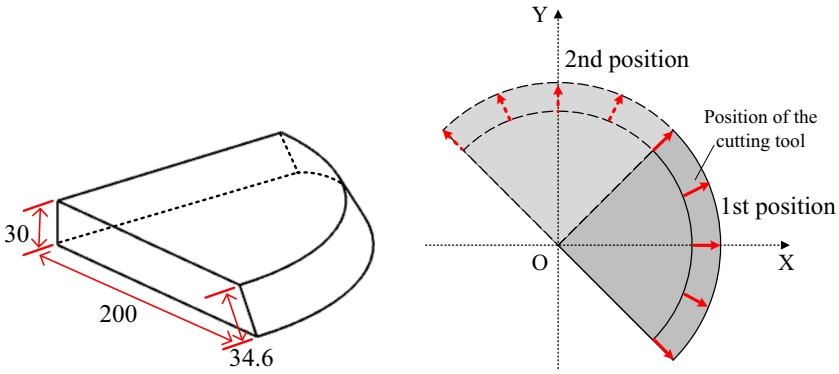

Fig. 9 The parameters and machining positions of 1/4 cone

(a) Parameters of the cone (b) The machining positions of the cone

200 mm. As displayed in Fig. 9, the 1/4 cone is placed at two different positions to make the sensitivity analysis. Since there are numerous cutting tool positions in the machining process, five cutting tool positions that are evenly distributed over the side surface are selected as the representative to perform sensitivity analysis of the machining error of the cone at different machining position. Based on the positions of the cutting tool, the positions of the five axes can be calculated as listed in Tables 3 and 4.

To determine the vital geometric errors that have major impacts on the machining error of the 1/4 cone, the LSA in which the sensitivity index is defined as LSIL is conducted. First, the effective cutting length can be calculated as 34.6 mm through the parameters of the 1/4 cone. Next, based upon the position of each axis and the normal vector of the side surface at each position of the cutting tool, the LSILs corresponding to the geometric errors at the five cutting tool positions can be calculated. By comparing the average value of the LSIL for each geometric error, the vital geometric errors can be distinguished. Since the vital geometric errors have the larger LSIL than the others, we can normalize the LSILs and use the pie chart to show their corresponding proportion to determine the vital geometric errors. It is more intuitive to use the pie chart to make the comparison, and the geometric errors corresponding to the larger sector area are identified as the vital geometric errors. The proportion of LSIL corresponding to each geometric error can be calculated by Eq. (15), where LSIL_i represents the calculated LSIL of the geometric error E_i and PL_i represents the corresponding proportion (Fig. 10).

$$PL_i = \frac{\mathrm{LSIL}_i}{\sum_{i=1}^{41} \mathrm{LSIL}_i} \tag{15}$$

From the simulation results, the vital geometric errors for the first machining position of the cone can be judged as the six geometric errors [S_{yz}, $\varepsilon_x(x)$, $\varepsilon_x(y)$, S_{xz}, $\varepsilon_y(y)$, $\varepsilon_y(x)$]. Similarly, the vital geometric errors for the second machining position of the cone can be decided as the seven geometric errors [S_{yz}, $\varepsilon_x(x)$, $\varepsilon_x(y)$, S_{xz}, $\varepsilon_y(y)$, $\varepsilon_y(x)$, $\varepsilon_y(A)$].

To test the sensitivity analysis effect, the geometric errors are compensated in three different methods to see their influence on the machining error. The first method is to reduce the values of these vital geometric errors to the half of the previous values and maintain the previous values of the other geometric errors. The second method is to maintain the values of the vital geometric errors and reduce the values of the other geometric errors to the half of the previous values. The final method is to reduce all the geometric errors to the half of their previous values. Figure 11a shows the results of the average machining error of the cone side surface at the first machining position under the influence of four different groups of geometric errors. The histogram "1" represents the machining error without compensation of the geometric errors, and "2, 3, and 4" represent the machining error under the influence of

Table 3 The positions of five axes for the first 1/4 cone position

Axis	Position 1	Position 2	Position 3	Position 4	Position 5
X (mm)	70.7	92.4	100	92.4	70.7
Y (mm)	− 70.7	− 38.3	0	38.3	70.7
Z (mm)	173.2	173.2	173.2	173.2	173.2
B (°)	− 22.2	− 28.1	− 30	− 28.1	− 22.2
A (°)	− 20.7	− 11.0	0	11.0	20.7

Table 4 The positions of five axes for the second 1/4 cone position

Axis	Position 1	Position 2	Position 3	Position 4	Position 5
X (mm)	70.7	38.3	0	− 38.3	− 70.7
Y (mm)	70.7	92.4	100	92.4	70.7
Z (mm)	173.2	173.2	173.2	173.2	173.2
B (°)	− 22.2	− 12.5	0	12.5	22.2
A (°)	20.7	27.5	30	27.5	20.7

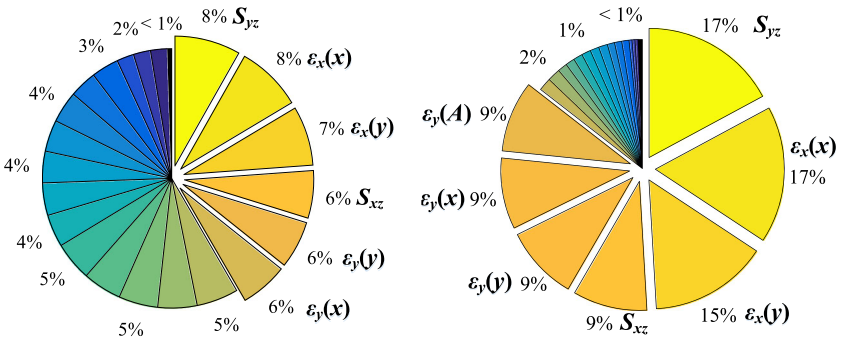

(a) The proportion of the LSILs for the first position 1/4 cone

(b) The proportion of the LSILs for the second position 1/4 cone

Fig. 10 The simulation result of the local sensitivity analysis

the geometric errors compensated through the above three different methods. When the geometric errors are compensated in different methods, the improvement of the machining error of the cone side surface is also different. Therefore, referring to histogram 1, the other histograms can be divided into two parts: unimproved part and improved part. The unimproved part of the histograms represent the actual average machining error of the cone side surface, while the improved part represent the improved machining error compared with the machining error without compensation of geometric errors. For example, when the geometric errors are compensated through the first method, compared with histogram 1, the machining error is improved by 0.123 mm that accounts for 21.4% of the total machining error as expressed in histogram 2. And the actual machining error is 0.574–0.123 = 0.451 mm. Similarly, the simulation results for the machining error of the cone side surface at the second machining position are displayed in Fig. 11b. In order to observe the improvement of the machining error of the cone side surface more intuitively, the simulation results are represented by the chromatograms. Figure 12a displays the machining error of the cone side surface when the geometric errors are not compensated. Its corresponding average machining error is the histogram 1 in Fig. 11a. The machining error of the cone side surface under the compensation of the vital geometric errors is shown in Fig. 12b that corresponds to histogram 2 in Fig. 11a. Similarly, the simulation results for the second machining position are displayed in Fig. 13.

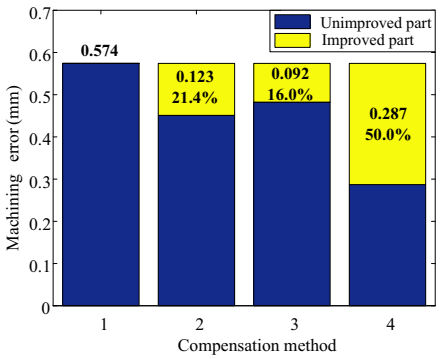

(a) The machining error under different compensation methods for the 1st machining position of the 1/4 cone side surface

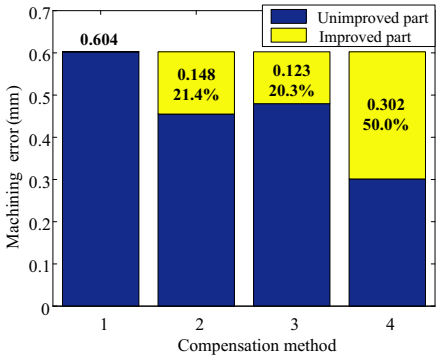

(b) The machining error under different compensation methods for the 2nd machining position of the 1/4 cone side surface

Fig. 11 Simulation results of the machining error by different compensation methods of geometric errors

The simulation results in Figs. 11, 12, and 13 have well examined the effectiveness of the LSA method using LSIL as the sensitivity index. As shown in Fig. 11, the machining error is improved by 0.123 and 0.148 mm through compensating the vital geometric errors, while the machining error is improved by 0.092 and 0.123 mm through compensating the other geometric errors. It can be observed that the machining error is more effectively improved by compensating the vital geometric errors than by compensating the other geometric errors. Considering that the number of the vital geometric errors for the two machining positions is 6 and 7, which is much smaller than the number of remaining geometric errors, it is more efficient to improve the machining error by compensating the vital geometric errors. By comparing the histograms 2 and 4 in Fig. 11, it can be seen that the improvement of the machining error is also appreciable by compensating the vital geometric errors compared with by compensating all 41 geometric errors. Moreover, as shown in Figs. 12 and 13, by contrasting to the machining error without compensation of geometric errors, the improvement of machining error by compensating vital geometric errors can be intuitively observed. After the compensation of the vital geometric errors, the machining error of the cone side surface has been well

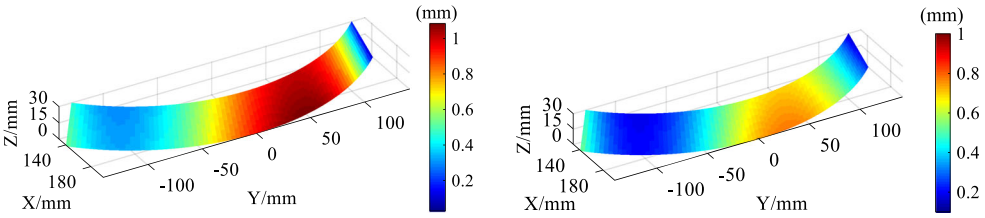

(a) The machining error without geometric errors compensation

(b) The machining error with vital geometric errors compensation

Fig. 12 The machining error of the 1/4 cone at the first machining position

reduced. Therefore, it denotes that the vital geometric errors identified by the LSA do have a greater impact on machining error than the other geometric errors. It can be concluded that the LSA method in which the sensitivity index is defined as LSIL is effective.

4.2 Global sensitivity analysis

To determine the vital geometric errors affecting the volumetric error in the whole workspace, the GSA is performed through applying the sensitivity index GSIL. The workspace of the five-axis machine tool is as introduced in Sect. 2.1; i.e., the strokes of the translational axes are $x \times y \times z = 5000 \times 2000 \times 500$ mm, and the strokes of the rotary axes are both [− 30°, 30°]. The length between the rotation center and cutting tool tip is set as 200 mm, and the effective cutting length is set as 30 mm. The geometric errors are set to the same values as in the numerical simulation in Sect. 4.1 (0.1 μm for the position errors and 0.1 μrad for the angular errors). Thus, the GSIL for each geometric error can be calculated by Eq. (14). Following the same method to address the LSILs in LSA, normalize the GSILs and use the pie chart to describe the proportion of the GSIL of each geometric error. As the same with Eq. (15), the proportion of GSIL corresponding to each geometric error can be calculated by Eq. (16), where GSIL_i represents the calculated GSIL of the geometric error E_i and PG_i represents the corresponding proportion.

$$PG_i = \frac{\mathrm{GSIL}_i}{\sum_{i=1}^{41} \mathrm{GSIL}_i} \tag{16}$$

The result is shown in Fig. 14. Because the vital geometric errors have the greater GSIL, the geometric errors corresponding to the larger sector area are identified as the vital geometric errors. From the result, the vital geometric errors can be obviously determined as $[S_{yz}, \varepsilon_x(x), S_{xy}, \varepsilon_z(x)]$.

ISO 230–6 defined a diagonal measurement by using a laser interferometer [31]. The cutting tool moves along each body diagonal of the workspace, and the diagonal displacements will be influenced by each geometric error. With reference to this method, nine points on the body diagonal of the workspace, as shown in Fig. 15, are selected to test the influence of the vital geometric errors on the error of the cutting tool. The points 1 to 8 are at the four equidistant distances of the body diagonals. Point 9 is at the center of the workspace.

The identified vital geometric errors by GSA are expected to have a significant influence on both the position and posture error of the cutting tool in the whole workspace. Thus, in the simulation, the position and posture error of the cutting tool are considered separately to test the influence of the identified vital geometric errors on them. Since the positions of the nine points in the workspace are determined, the positions of translational axes for the points can be obtained. The average error of the cutting tool for the nine points under the whole motion range of the two rotary axes can be simulated, which can approximately denote the influence of the geometric errors on the whole workspace. Using the same method in Sect. 4.1 to test the GSA effect, the position and posture error of the cutting tool are calculated when the geometric errors are compensated in three different methods. The position and posture error of the cutting tool are simulated under the influence of four different groups of geometric errors, and the simulation results are displayed in Figs. 16, 17, and 18. Like the method to describe the simulation results as Fig. 11, the

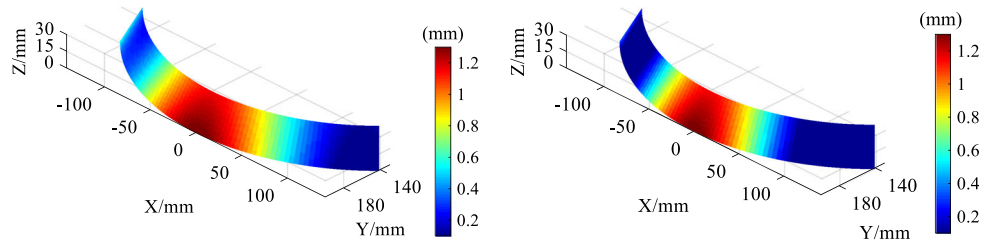

(a) The machining error without geometric errors compensation

(b) The machining error with vital geometric errors compensation

Fig. 13 The machining error of the 1/4 cone at the second machining position

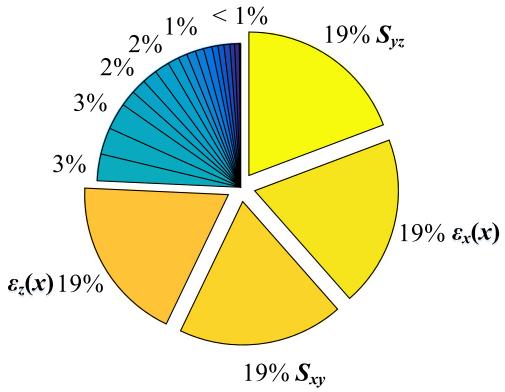

Fig. 14 The simulation result of the global sensitivity analysis

average position and posture error of the cutting tool are listed by histograms in Fig. 16. As the same, comparing to the histogram representing the error of the cutting tool without geometric error compensation, the other histograms are divided into the unimproved and improved parts. In order to observe the improvement of the error of the cutting tool intuitively, the contour map is used to illustrate the simulation results. Figure 17a shows the average position error of nine points within the motion range of rotary axes *A* and *B*, when the geometric errors are not compensated. Figure 17b shows the result after compensating the vital geometric errors. Similarly, the simulation results of posture error without and with vital geometric errors compensation are displayed in Fig. 18.

From the results as shown in Fig. 16a, it can be observed that the improvement of the position error with vital geometric errors compensation is 0.259 mm, which is close to the result (0.268 mm) with compensation of all the geometric errors. Considering that the number of the vital geometric errors identified by GSA is only 4 (S_{yz}, $\varepsilon_x(x)$, S_{xy}, $\varepsilon_z(x)$), the improvement of the position error of the cutting tool is very effective. This result can also be intuitively seen in Fig. 17, where Fig. 17a corresponds to histogram 1 in Figs. 16a and 17b correspond to histogram 2 in Fig. 16a. The position error of the cutting tool within the motion range of rotary axes *A* and *B* [− 30°, 30°] is smaller when vital geometric errors are compensated than when geometric errors are not compensated. From the results as shown in Figs. 16b and 18, the posture error of the cutting

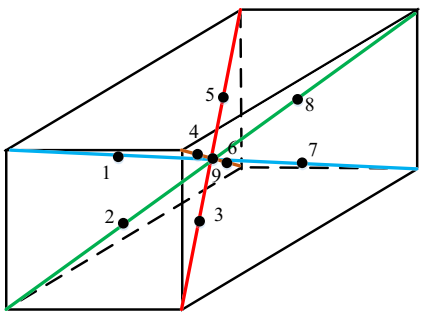

Fig. 15 The nine positions selected in the workspace

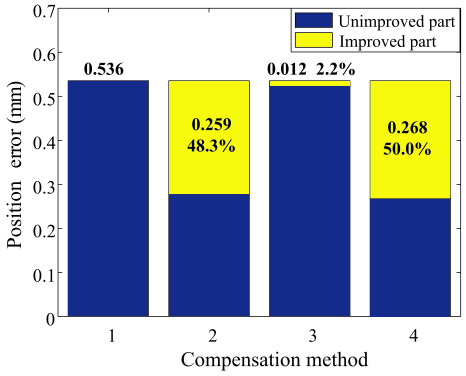

(a) The average position error of the cutting tool under different compensation methods

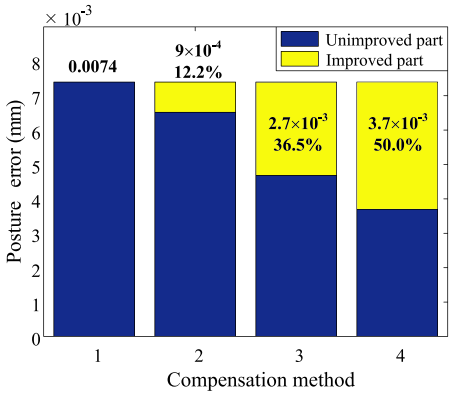

(b) The average posture error of the cutting tool under different compensation methods

Fig. 16 The average tool errors under different compensation methods

tool with vital geometric errors compensation seems to change little. Considering that the vital geometric errors account for 4/41 = 9.8% of the total geometric errors, while the improvement of the posture error by compensating the vital geometric errors accounts for 0.0009/0.0037 = 24.3% of the improvement of the posture error by compensating all the geometric errors, the improvement of the posture error by compensating the vital geometric errors is more effective. Summarized above, the vital geometric errors identified by the GSA are demonstrated to have a greater influence on the error of the cutting tool. It can be concluded that the GSA method in which the sensitivity index is defined as GSIL is effective.

5 Discussion

The simulations for the LSA and GSA are under the assumption that all the geometric errors are fixed values. This assumption is the same as in precision design. When the actual measurement data of the geometric errors are obtained, the proposed SA method is also applicable because the calculation of LSIL and GSIL is based on the volumetric error model. Hence, the proposed SA method is suitable for both precision design and error compensation of the machine tools.

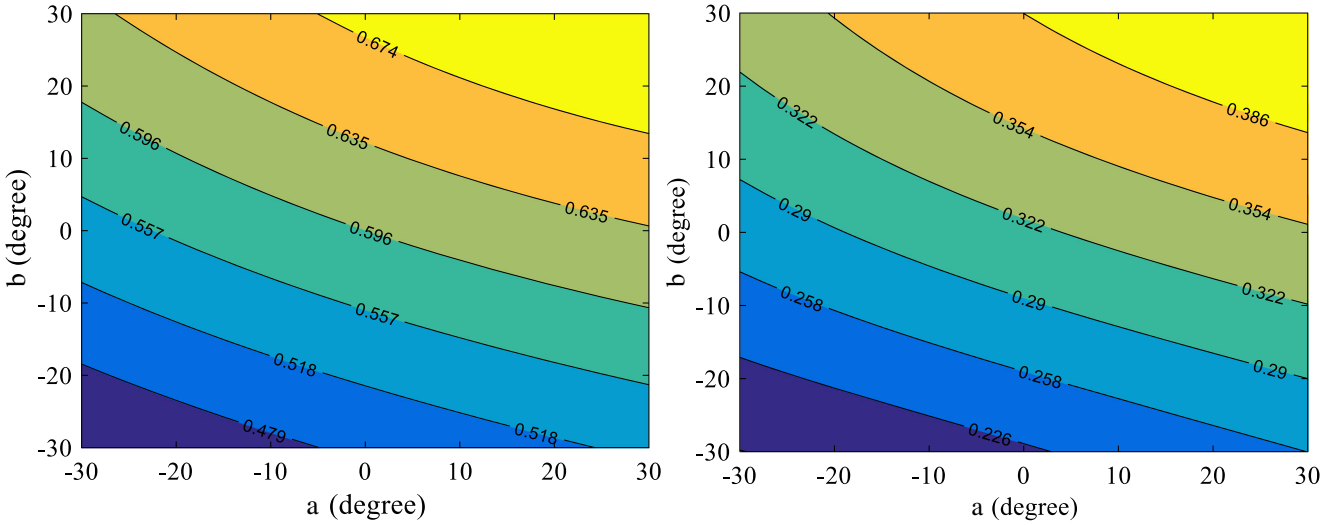

(a) The average position error of the cutting tool without geometric errors compensation (mm)

(b) The average position error of the cutting tool with vital geometric errors compensation (mm)

Fig. 17 The average position error of the cutting tool (**a**) The average position error of the cutting tool without geometric errors compensation (mm) (**b**) The average position error of the cutting tool with vital geometric errors compensation (mm)

In Sect. 4.1, the vital geometric errors for the two machining positions of the 1/4 cone identified by the LSA are nearly the same. The first six geometric errors ranked by the proportion of LSIL are both [S_{yz}, $\varepsilon_x(x)$, $\varepsilon_x(y)$, S_{xz}, $\varepsilon_y(y)$, $\varepsilon_y(x)$]. However, for the two different machining positions, the proportions of the first six geometric errors have a big difference, because the definition of the LSIL is related to the positions of the cutting tool and the workpiece surface. As illustrated in Fig. 10, the proportion of the vital geometric errors for the second machining position is much larger than the ones for the first position, but the improvement of the machining error has only increased a little as shown in Fig. 11. This issue can be explained based on the definition of the LSIL. From Eq. (12), it can be known that the LSIL can only represent the size of the effect of the geometric error on the error of the cutting tool, but not the direction. As shown in Fig. 19, suppose that **OP** and **PQ** are the position error vectors caused by two error components, the final position error vector will be **OQ**. When **OP** is reduced to half its size, the final position error vector will be $\mathbf{OQ_1}$. When **PQ** is reduced to half its size, the final position error vector will be $\mathbf{OQ_2}$. Obviously, the size of $\mathbf{OQ_2}$ is smaller than the size of **OQ**, and the size of $\mathbf{OQ_1}$ is larger than the size of **OQ**. This

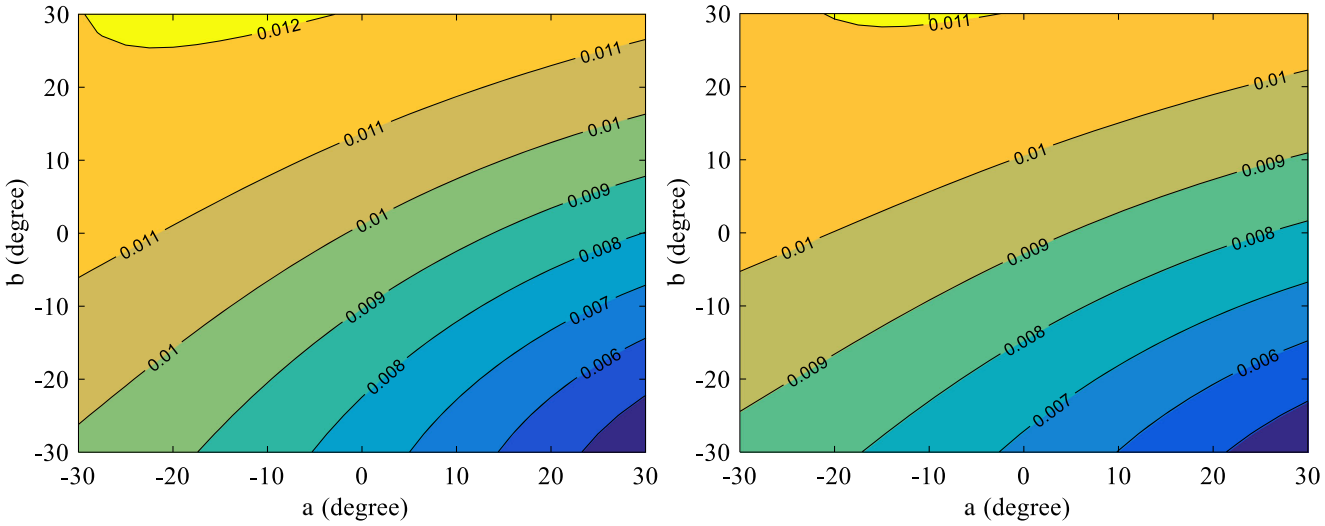

(a) The average posture error of the cutting tool without geometric errors compensation

(b) The average posture error of the cutting tool with vital geometric errors compensation

Fig. 18 The average posture error of the cutting tool (**a**) The average posture error of the cutting tool without geometric errors compensation (**b**) The average posture error of the cutting tool with vital geometric errors compensation

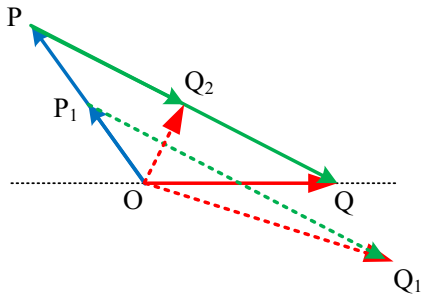

Fig. 19 The relationship between the position error vector caused by error components and the final position error vector

result is related to the directions of these position error vectors. Therefore, though the vital geometric errors have significant influences on the position error of the cutting tool, the same reduction of their size may not lead a significant improvement of the error of the cutting tool.

For the GSA in Sect. 4.2, as displayed in Fig. 16, the improvement of the position error (48.3%) is much better than the posture error (12.2%). As introduced in Sect. 3.2, if the position error transformation vector of one geometric error has no relationship with the length L, this geometric error has no influence on the posture error of the cutting tool. Because the position error caused by this geometric error is equal at any position over the cutting tool, which just leads to an offset of the cutting tool. There are 20 out of 41 geometric errors with such a property as displayed in Table 2. If the vital geometric errors are among these 20 geometric errors, the reduction of the vital geometric errors will have no influence on the improvement of posture error. In addition, from Eq. (13) and Fig. 7, it can be recognized that W_i mainly reflects the level of the difference between the actual and the ideal position of the cutting tool in the workspace. The reduction of the position error over the effective cutting length will certainly decrease this difference, while the reduction of the posture error may not. As shown in Fig. 5, the $\mathbf{O_1P_{a1}}$ and $\mathbf{O_2P_a}$ have the same posture error, but the position error of $\mathbf{O_1P_{a1}}$ is smaller than $\mathbf{O_2P_a}$. Thus, the influence of the vital geometric errors on the error of the cutting tool is mainly reflected on the position error.

For the five-axis machine tool that is the research target of this study, the vital geometric errors identified by either LSA or GSA are all angular errors, i.e., [S_{yz}, $\varepsilon_x(x)$, $\varepsilon_x(y)$, S_{xz}, $\varepsilon_y(y)$, $\varepsilon_y(x)$, $\varepsilon_y(A)$] and [S_{yz}, $\varepsilon_x(x)$, S_{xy}, $\varepsilon_z(x)$]. And among the vital geometric errors, the PIGEs between the three translational axes occupy a large proportion. Since the five-axis machine tool is a series structure and there exists the cutting tool length, the influence of the geometric errors that belong to angular errors on the error of the cutting tool will be amplified with the movement of the machine tool. The geometric errors S_{xy}, S_{xz}, and S_{yz} representing the squareness between the three translational axes are also angular errors; they directly affect the relative motion accuracy of two adjacent translational axes. And as the range of relative motion increases, the influence of S_{xy}, S_{xz}, and S_{yz} on the motion accuracy of the machine tool will also be increased. Therefore, for the precision design and error compensation of five-axis machine tools, the geometric errors belong to angular errors should be paid more attention, especially the PIGEs between translational axes.

6 Conclusion

In order to improve the accuracy of the five-axis machine tool, compensating the geometric errors is an important method. Moreover, the accuracy improvement is more effective through compensating the vital geometric errors that have major influence on the volumetric error. Therefore, this paper presents a sensitivity analysis method to determine the vital geometric errors by defining new sensitivity indices.

1. Based on the MBS method, the volumetric error model of the five-axis machine tool with 41 geometric errors is established. The new sensitivity indices are defined based on the volumetric error model and the introduction of effective cutting length, i.e., LSIL for LSA and GSIL for GSA. The definition of new sensitivity indices has considered both the position and posture error of the cutting tool, which addresses the problem of there are too many sensitivity indices in conventional sensitivity analysis method.
2. The LSA and GSA are conducted in which the LSIL and GSIL are used. In the LSA for the 1/4 cone at two different machining positions, the machining error has improved by 21.4 and 24.5% by compensating six and seven identified vital geometric errors, compared with 16.0 and 20.3% by compensating the other geometric errors. In the GSA, the position and posture error of the cutting tool have improved by 48.3 and 12.2% by compensating four identified vital geometric errors. The simulation results have well proven the validity of the proposed sensitivity analysis method.
3. From the sensitivity analysis results of the five-axis machine tool, we can see that the vital geometric errors which have significant influence on the error of the cutting tool are all angular errors. Therefore, in the improvement of the five-axis machine tool accuracy, more attention should be paid to the control of the geometric errors that belong to the angular error, especially the PIGEs between the three translational axes: S_{xy}, S_{xz}, and S_{yz}.

Acknowledgements This research is supported by the National Key Scientific and Technological Project (Grant No. 2015ZX04001002).

References

1. Ramesh R, Mannan MA, Poo AN (2000) Error compensation in machine tools - a review Part I: Geometric, Cutting Force induced and fixture depend errors. Int J Mach Tools Manuf 40(9):1235–1256
2. Khan AW, Chen W (2011) A methodology for systematic geometric error compensation in five-axis machine tools. Int J Adv Manuf Technol 53(5):615–628
3. Liu H, Li B, Wang X, Tan G (2011) Characteristics of and measurement methods for geometric errors in CNC machine tools. Int J Adv Manuf Technol 54(1–4):195–201
4. Nojedeh MV, Habibi M, Arezoo B (2011) Tool path accuracy enhancement through geometrical error compensation. Int J Mach Tools Manuf 51(6):471–482
5. Schwenke H, Knapp W, Haitjema H, Weckenmann A, Schmitt R, Delbressine F (2008) Geometric error measurement and compensation of machines-an update. CIRP Ann - Manuf Technol 57(2):660–675
6. Xu Y, Zhang L, Wang S, Du H, Chai B, Hu SJ (2015) Active precision design for complex machine tools : methodology and case study. Int J Mach Tools Manuf 80(1):581–590
7. Cui G, Lu Y, Li J, Gao D (2012) Geometric error compensation software system for CNC machine tools based on NC program reconstructing. Int J Adv Manuf Thechnol 63(1–4):169–180
8. Cui G, Lu Y, Gao D, Yao Y (2012) A novel error compensation implementing strategy and realizing on Siemens 840D CNC systems. Int J Mach Tools Manuf 61(5–8):595–608
9. Creamer J, Bristow DA, Landers RG (2017) Selection of limited and constrained compensation tables for five-axis machine tools. Int J Adv Manuf Technol 92:1315–1327
10. Donmez MA, Blomquist DS, Hocken RJ, Liu CR, Barash MM (1986) A general methodology for machine tool accuracy enhancement by error compensation. Precis Eng 8(4):187–196
11. Fu G, Fu J, Gao H, Yao X (2017) Squareness error modeling for multi-axis machine tools via synthesizing the motion of the axes. Int J Adv Manuf Technol 89(9):2993–3008
12. Chen GS, Mei XS, Li HL (2013) Geometric error modeling and compensation for large-scale grinding machine tools with multi-axes. Int J Adv Manuf Technol 69(9–12):2583–2592
13. Lee JH, Liu Y, Yang SH (2006) Accuracy improvement of miniaturized machine tool: geometric error modeling and compensation. Int J Mach Tools Manuf 46(12–13):1508–1516
14. Zhu S, Ding G, Qin S, Lei J, Zhuang L, Yan K (2012) Integrated geometric error modeling, identification and compensation of CNC machine tools. Int J Mach Tools Manuf 52(1):24–29
15. Zhang Z, Liu Z, Cheng Q, Qi Y, Cai L (2017) An approach of comprehensive error modeling and accuracy allocation for the improvement of reliability and optimization of cost of a multi-axis NC machine tool. Int J Adv Manuf Technol 89(1):561–579
16. Zhu W, Wang Z, Yamazaki K (2010) Machine tool component error extraction and error compensation by incorporating statistical analysis. Int J Mach Tools Manuf 50(1):798–806
17. Zhang H, Yang J, Zhang Y, Shen J, Wang C (2011) Measurement and compensation for volumetric positioning errors of CNC machine tools considering thermal effect. Int J Adv Manuf Technol 55(1):275–283
18. He Z, Fu J, Zhang X, Shen H (2016) A uniform expression model for volumetric errors of machine tools. Int J Mach Tools Manuf 100:93–104
19. Saltelli A, Ratto M, Tarantola S, Campolongo F (2006) Sensitivity analysis practices : strategies for model-based inference. Reliab Eng Syst Saf 91(10–11):1109–1125
20. Wang S, Ehmann KF (1999) Measurement methods for the position errors of a multi-axis machine. Part 1 : principles and sensitivity analysis. Int J Mach Tools Manuf 39(6):951–964
21. Fan K, Wang H, Zhao J, Chang T (2003) Sensitivity analysis of the 3-PRS parallel kinematic spindle platform of a serial-parallel machine tool. Int J Mach Tools Manuf 43(15):1561–1569
22. Chen G, Liang Y, Sun Y, Chen W, Wang B (2013) Volumetric error modeling and sensitivity analysis for designing a five-axis ultra-precision machine tool. Int J Adv Manuf Technol 68(9–12):2525–2534
23. Li J, Xie F, Liu XJ (2016) Geometric error modeling and sensitivity analysis of a five-axis machine tool. Int J Adv Manuf Technol 82(9):2037–2051
24. Cheng Q, Zhao H, Zhang G (2014) An analytical approach for crucial geometric errors identification of multi-axis machine tool based on global sensitivity analysis. Int J Adv Manuf Technol 75(1–4):107–121
25. Cheng Q, Feng Q, Liu Z, Gu P, Zhang G (2016) Sensitivity analysis of machining accuracy of multi-axis machine tool based on POE screw theory and Morris method. Int J Adv Manuf Technol 84(9–12):2301–2318
26. Cheng Q, Sun B, Liu Z, Li J, Dong X, Gu P (2017) Key geometric error extraction of machine tool based on extended Fourier amplitude sensitivity test method. Int J Adv Manuf Technol 90(9–12):3369–3385
27. Zhang X, Zhang Y, Pandey MD (2015) Global sensitivity analysis of a CNC machine tool : application of MDRM. Int J Adv Manuf Technol 81(1–4):159–169
28. Guo S, Jiang G (2017) Investigation of sensitivity analysis and compensation parameter optimization of geometric error for five-axis machine tool. Int J Adv Manuf Technol 93(1):3229–3243
29. Lee DM, Zhu Z, Lee KI, Yang SH (2011) Identification and measurement of geometric errors for a five-axis machine tool with a tilting head using a double ball-bar. Int J Precis Eng Manuf 12(2):337–343
30. International Standards Organization (ISO). ISO 230–7: Test code for machine tools, Part 7: Geometric accuracy of axes of rotation, 2006
31. International Standards Organization (ISO). ISO 230–6: Test code for machine tools, Part 6: Determination of positioning accuracy on body and face diagonals (Diagonal displacement tests), 2002